

Figure 2.2 Two-mass model of the vocal folds, showing compliances coupling the two masses to the lateral walls and to each other.

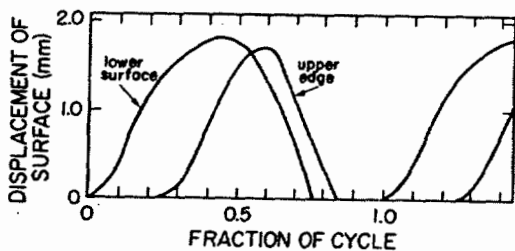


Figure 2.1 The upper part of the figure shows estimated lateral sections through the vibrating vocal folds at eight equally spaced times through the glottal vibration cycle. Data were obtained by Baer (1975) from an excised dog larynx. The scale of 1 mm is indicated by horizontal and vertical lines in the upper right of each panel. The curves in the lower panel show the lateral width of the glottal opening measured at the upper edge of the vocal folds and at a point 1.3 mm below the upper edge. These curves illustrate the time lag between the displacements of the lower and upper portions of the vocal folds. (From Baer, 1975.)

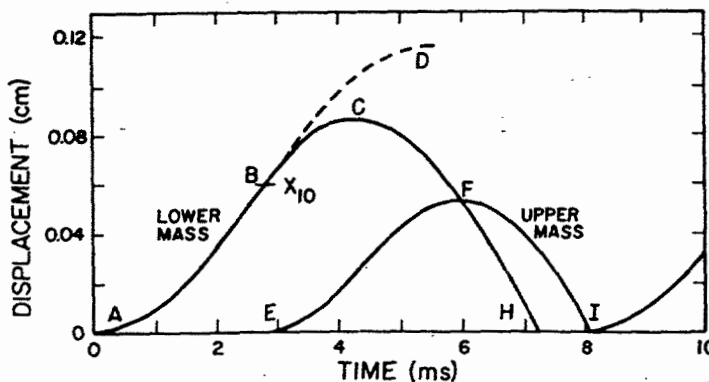


Figure 2.4 Schematic representation of the motion of lower and upper masses during a cycle of vibration of the two-mass model in figure 2.2. The displacement of the lower mass is given by ABCFH, whereas the trajectory of the upper mass is EFI. The upper mass begins its lateral motion at E, when the displacement of the upper mass is  $x_{10}$ . The dashed line to point D is the projected trajectory of the lower mass if the glottis did not open and if steady pressure on the lower mass were maintained. The glottis is open and airflow occurs in the region marked by the line EFH. The beginning of the second cycle is shown at the right. Assumed physical parameters of vocal folds are appropriate for an adult male, as described in the text.

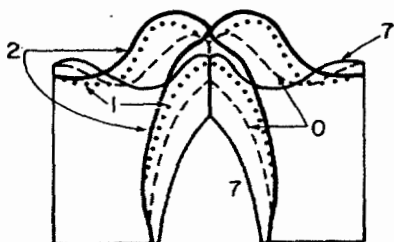


Figure 2.3 Tracings of vocal fold shapes at four instants of time during the closed phase, from figure 2.1. (From Baer, 1975.)

G2

Model

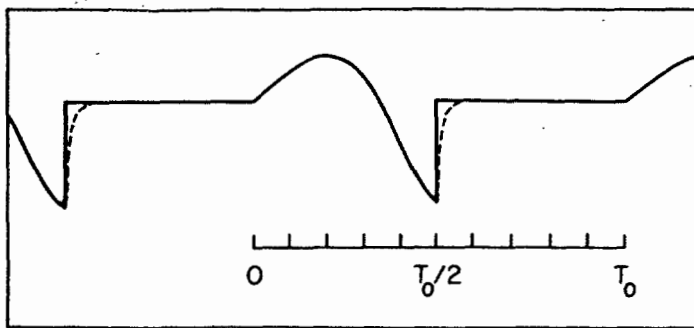


Figure 2.28 Waveform of derivative of glottal airflow  $U_g$  based on the LF model (Fant et al., 1985). The period is  $T_0$  and the open quotient  $OQ = 50$  percent. The solid line is for an abrupt discontinuity in the derivative of  $U_g$  (i.e., parameter  $T_2 = 0$ ) and the dashed line corresponds to  $T_2 = 0.025 T_0$ . See text.

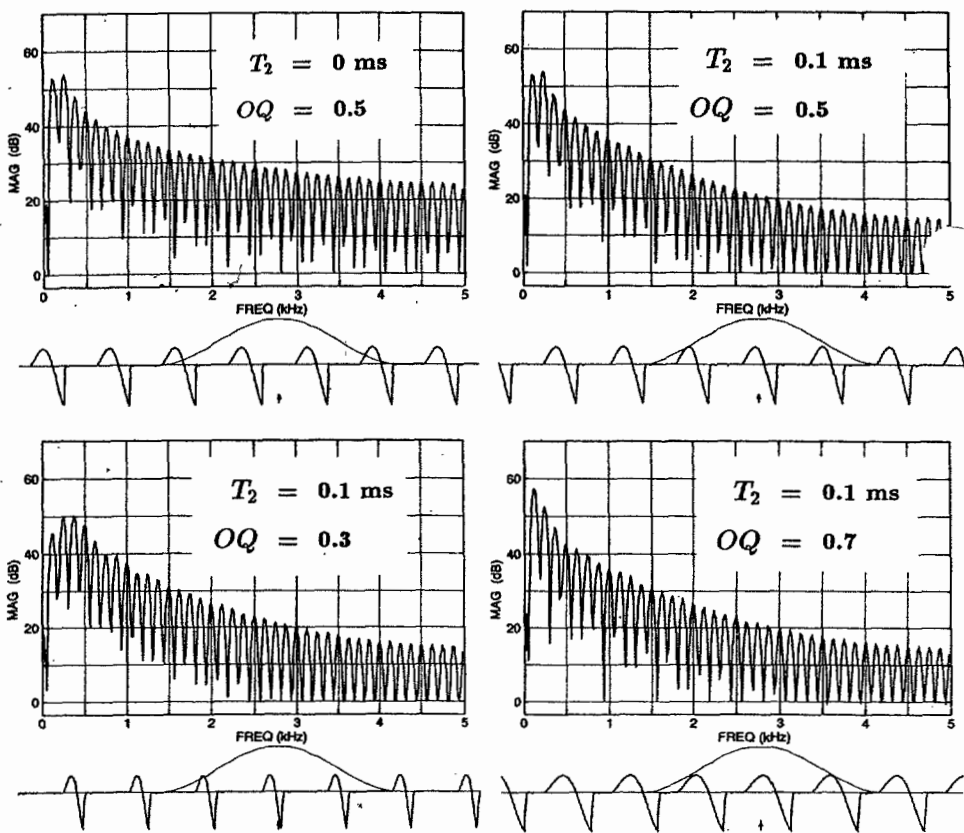
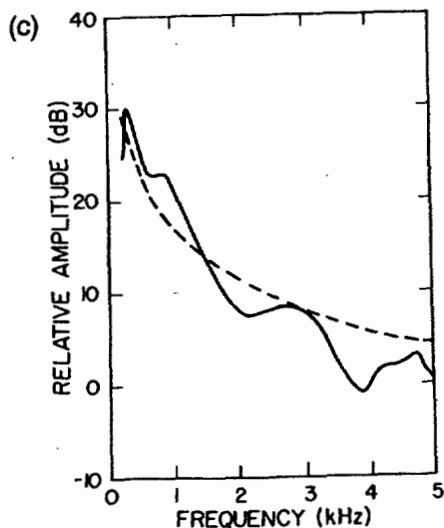
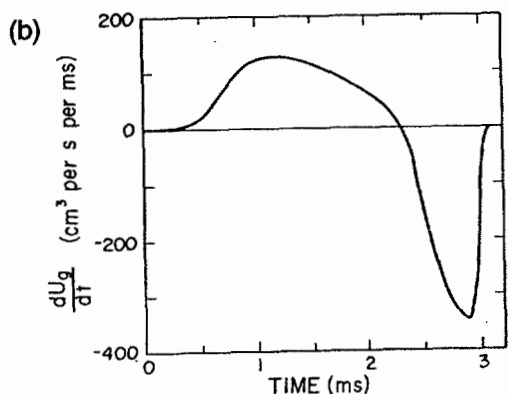
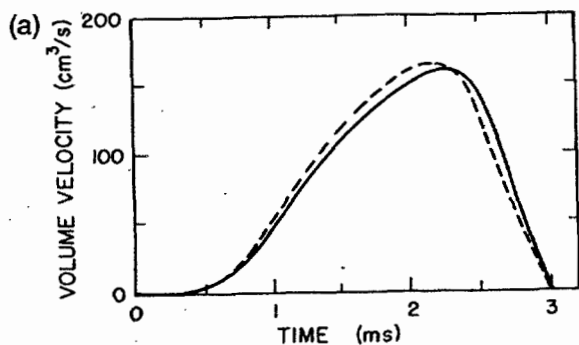


Figure 2.29 Spectrum of derivative of glottal airflow for LF model for several combinations of values of return time  $T_2$  and open quotient  $OQ$  as indicated. Fundamental frequency = 125 Hz. These spectra were calculated from a version of the LF model developed by Dennis Klatt (Klatt and Klatt, 1990).

Figure 2.12 (a) The solid line is the volume velocity waveform corresponding to the model with increased stiffness, for which displacements of masses are as shown in figure 2.11, and supra- and subglottal configurations are as in figure 2.8. The dashed line corresponds to the waveform in the absence of the effect of supra- and subglottal acoustic masses. (b) Derivative of waveform given by solid line in (a). (c) Spectrum of  $dU_g/dt$  in (b). The dashed line has a  $-6$  dB per octave slope.

WYI  
Glides



Figure 9.19 Midsagittal sections when the vocal tract reaches its most constricted configuration for the glides /w/ (left) and /j/ (right). In the case of /w/, the frontal lip contour is also shown, to illustrate the lip rounding. (Adapted from Bothorel et al., 1986.)

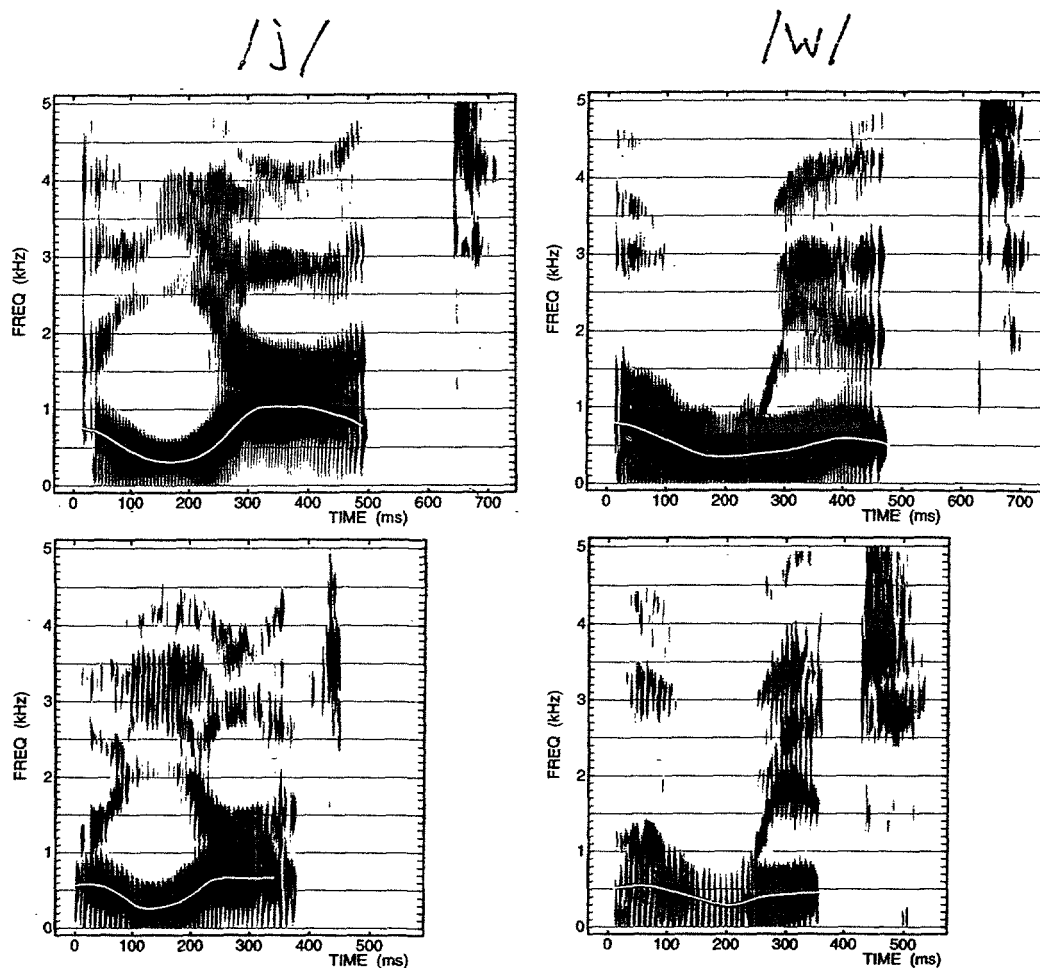


Figure 9.24 Spectrograms of the utterances /ə'jat/ and /ə'wit/ produced by a female speaker (top) and a male speaker (bottom). Measured F1 trajectories are superimposed on the spectrograms.

WY 2  
female /əwit/

male

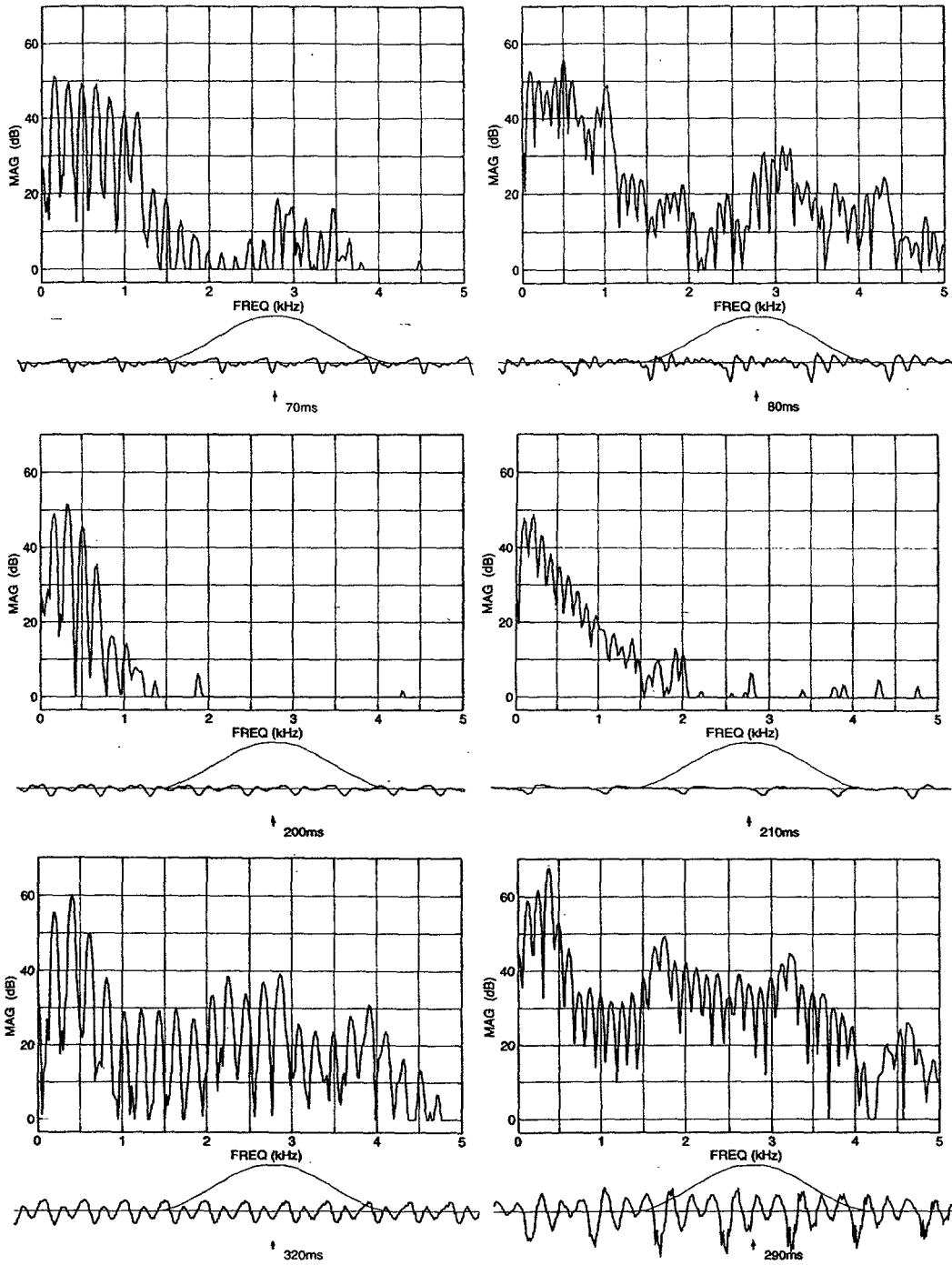


Figure 9.27 Spectra sampled at several points through the utterance /əwit/, produced by a female speaker (left) and a male speaker (right). In each case, the spectrum in the middle is sampled near the point of maximum constriction, and the spectra on the top and bottom are sampled in the preceding unstressed vowel and the following stressed vowel, respectively. Waveforms and time windows (30 ms) are shown below the spectra.

WY3

/ə'jat/

female

male

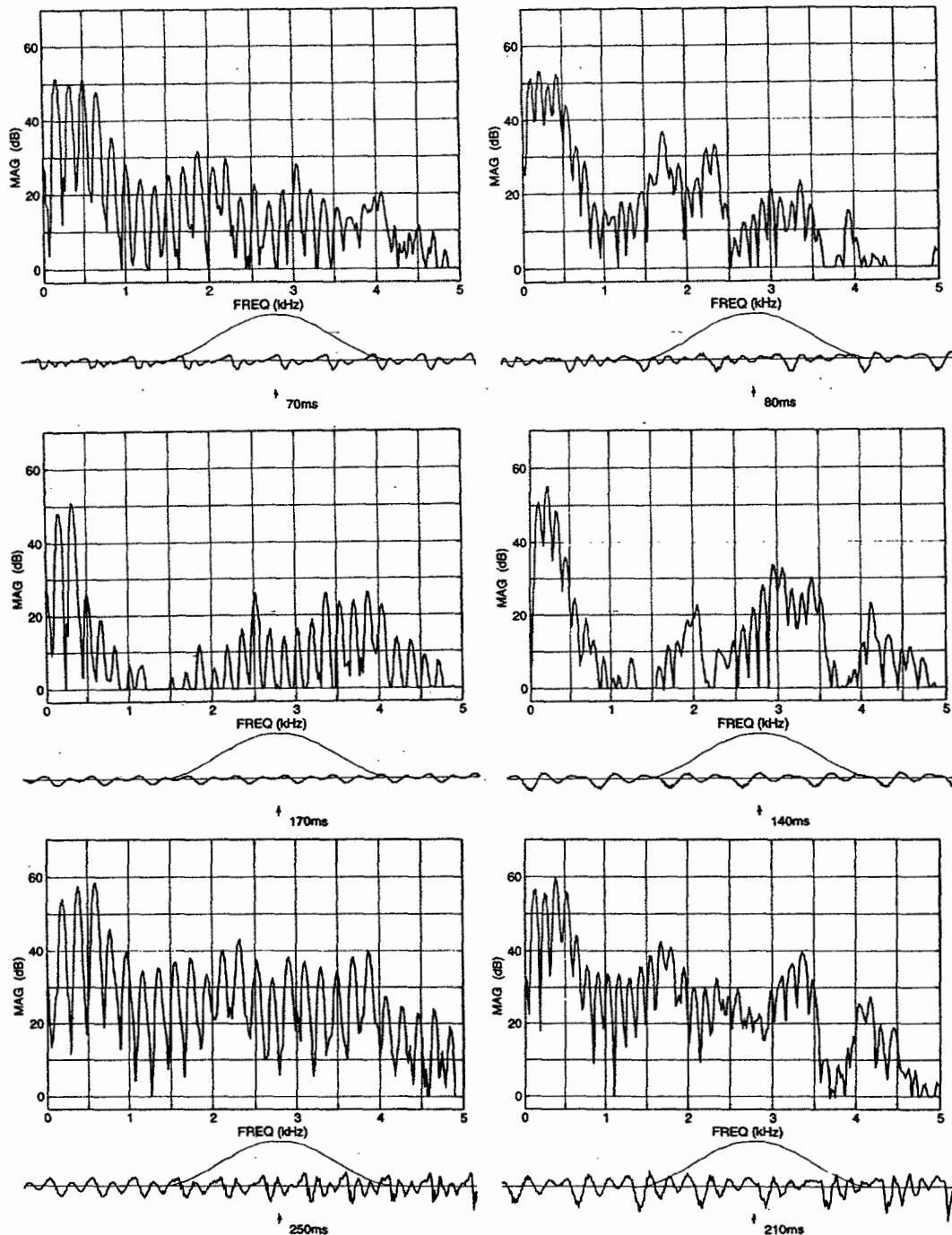
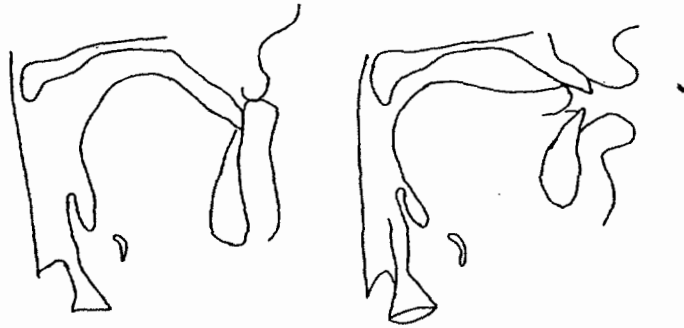


Figure 9.33 Same as figure 9.27, except that the utterance is /ə'jat/. The female speaker is represented in the left panels and the male speaker in the right panels.

N1

# Nasal consonants



**Figure 9.1** Midsagittal sections through the vocal tract during the production of nasal consonants produced by closing the lips (left) and raising the tongue tip to the alveolar ridge (right). For the labial consonant, the context is "Mets tes beaux habits," and for the alveolar consonant the context is "Une réponse ...." (Adapted from Bothorel et al., 1986.)

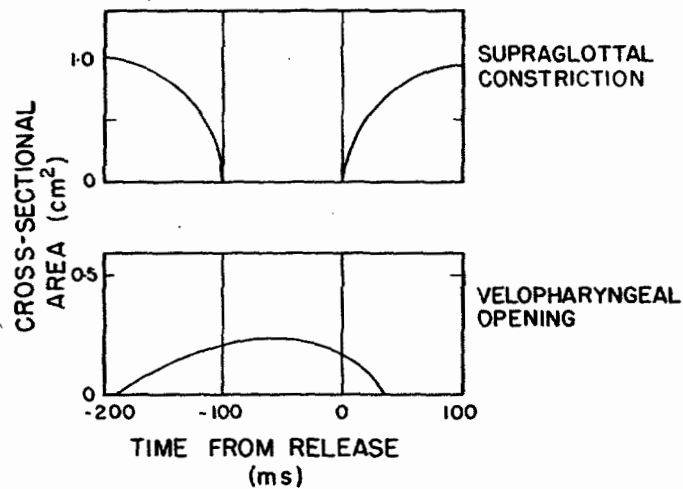


**Figure 9.2** Schematization of the time course of the cross-sectional area of the oral constriction (upper panel) and of the velopharyngeal opening (lower panel) during production of a nasal consonant in intervocalic position. The detailed shapes of these trajectories depend on the place of articulation for the consonant and for the adjacent sounds.

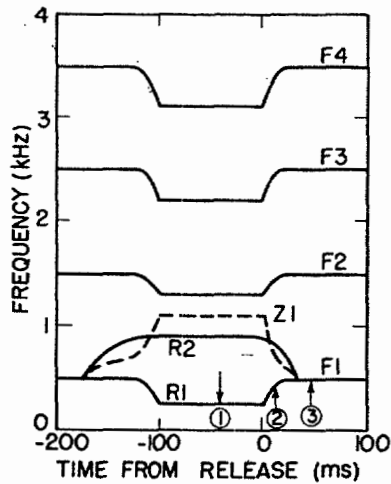


**Figure 9.5** Schematization of trajectories of poles and zeros of the transfer function of the vocal tract for a labial nasal consonant in intervocalic position. The transfer function is the ratio of the total volume velocity from the nose and mouth to the volume velocity at the glottis. The labial closure occurs between 0 and -100 ms on the abscissa. The lowest zero is labeled as Z1, and is shown as a dashed line. Zeros above Z1 are not shown. Poles are indicated by solid lines, including the two low-frequency poles R1 and R2 that replace the first formant during the interval when the velopharyngeal port is open. For times remote from the closure, poles and zeros due to acoustic coupling to the nasal cavity are canceled, and only the natural frequencies of the oral cavity remain, labeled F1 through F4. The vowel configuration is taken to have a uniform cross-sectional area. The points labeled 1, 2, and 3 indicate times at which the spectrum envelopes in figure 9.6 are calculated.

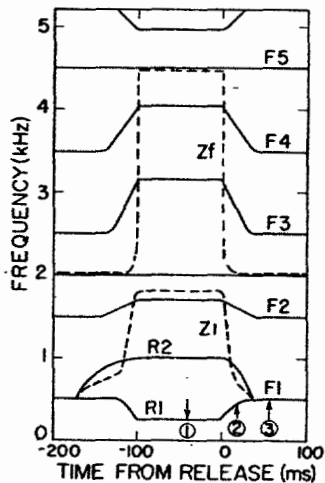


**Figure 9.9** Estimated trajectories of poles and zeros of the transfer function of the vocal tract for an alveolar nasal consonant in intervocalic position. Poles and zeros are labeled as in figure 9.5. The zero Zf accounts for acoustic coupling to the front cavity during the nasal murmur, as discussed in the text. The points labeled 1, 2, and 3 indicate times at which the spectrum envelopes in figure 9.10 are calculated.

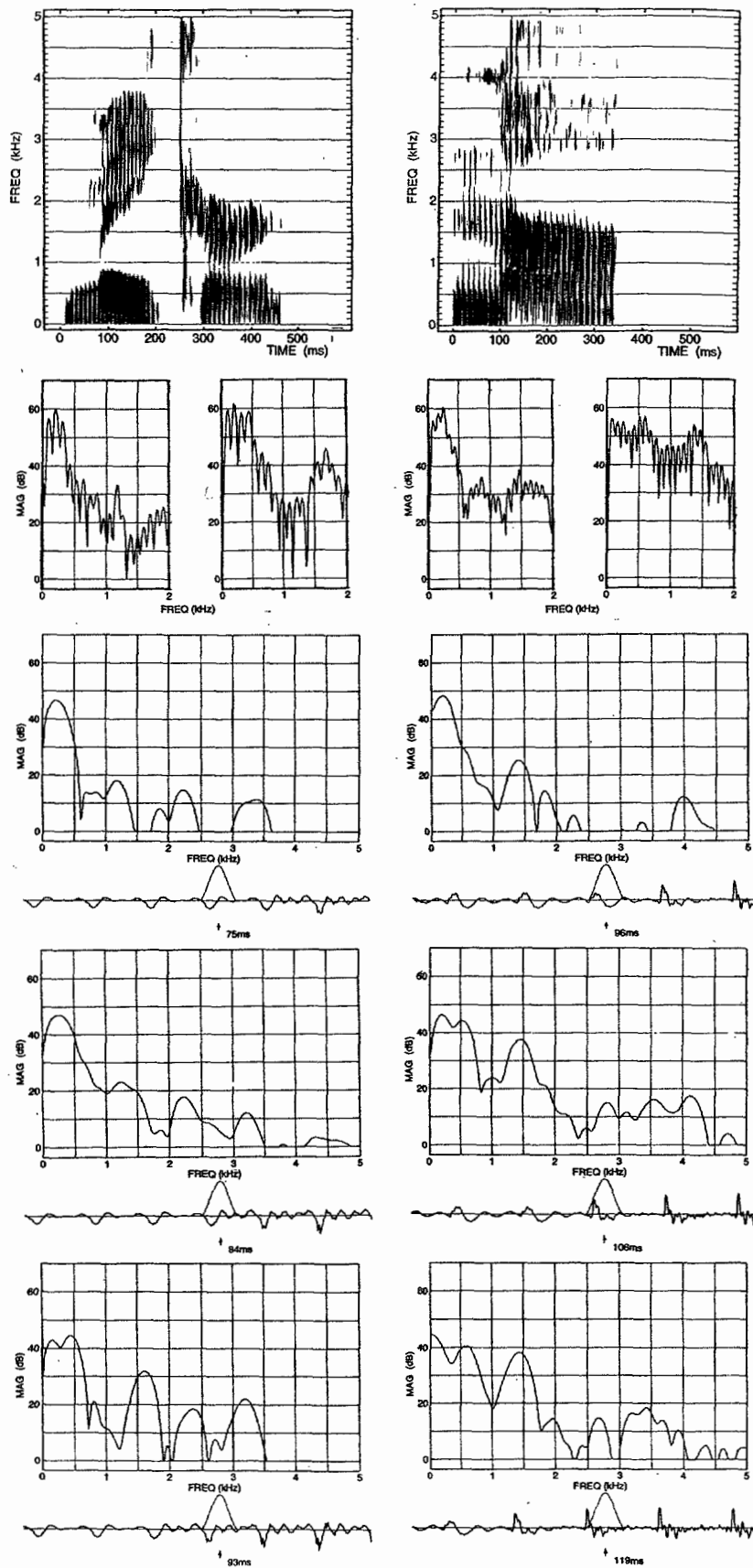


Figure 9.4 Spectrograms of the word *maker* (left) and the syllable */na/* (right) produced by two different male speakers are shown at the top. The two low-frequency spectra immediately below each spectrogram (time window = 26 ms) are sampled in the nasal murmur (left spectrum) and soon after the consonant release (right spectrum). The bottom three spectra in each column were sampled with a time window of 6.4 ms (as shown on the waveform in each case) as  $\alpha$  itered on three successive glottal periods immediately before the consonant release and just after the release. See text.

N4

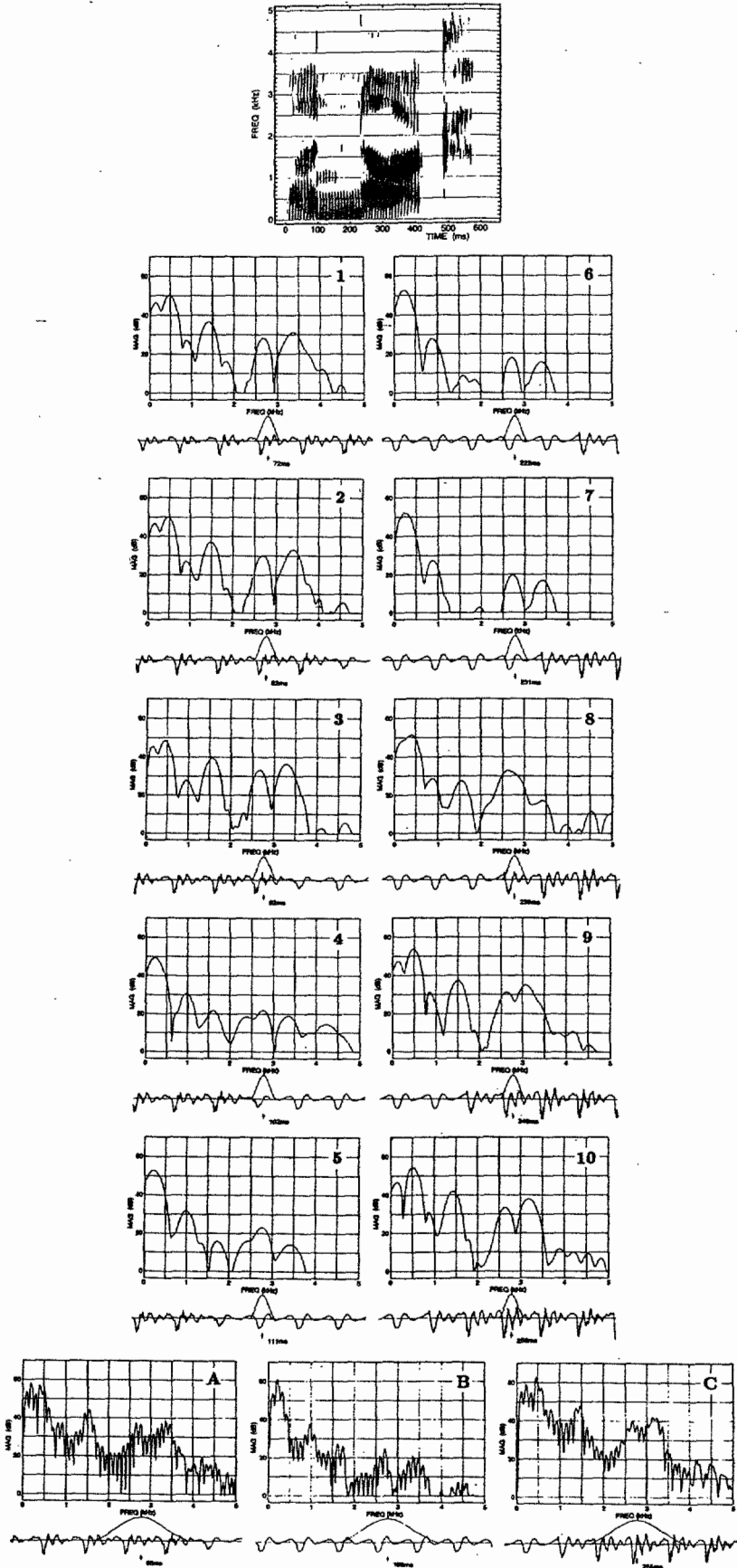


Figure 9.11 Acoustic data obtained from an alveolar nasal consonant /n/ in the utterance *a knock*. A spectrogram of the utterance is shown at the top, and the panels below the spectrogram are spectra sampled at several points and with different time windows. The sampling times and windows are as described in the legend for figure 9.7.